Quest Journals
Journal of Research in Applied Mathematics
Volume 11 ~ Issue 5 (May 2025) pp: 88-99
ISSN (Online): 2394-0743 ISSN (Print): 2394-0735
www.questjournals.org

Review Paper

The Impact of Climate Change on Groundwater Level decline: A Fractional Variable-Order Model

T.Saradhadevi, A.Kalavathi

[1]*(Research Scholar, Department of Mathematics, Sri GVG Visalakshi College for Women, India)*
[2]*(Assistant Professor, Department of Mathematics, Sri GVG Visalakshi College for Women, India)*
Corresponding Author: T.Saradhadevi

ABSTRACT: *Groundwater is a critical component of the Earth's freshwater resources, constituting approximately 30% of the world's freshwater supply. It is stored in aquifers and is indispensable for a variety of human purposes, such as agriculture, potable water supplies, and industrial operations. Groundwater declination has profound implications, including water scarcity, land subsidence, deteriorating water quality, and the disruption of ecosystems dependent on stable water tables. This paper proposes a nonlinear fractional variable-order model of groundwater declination in the sense of Liouville-Caputo(LC), Caputo-Fabrizio(CF) and Atangana –Baleanu (AB) fractional derivatives. The existence and uniqueness of fractional solutions has been established and numerical simulations have been carried out to illustrate the impact of pollution, deforestation, frequent pumping of water and evaporation on the groundwater level*.

KEYWORDS: *Groundwater, Fractional variable-order model, Liouville-Caputo, Caputo-Fabrizio, Atangana-Baleanu.*

R*eceived 11 May., 2025;* ***R****evised 20 May., 2025;* ***A****ccepted 22 May., 2025*

I. INTRODUCTION

Groundwater depletion is an increasingly critical issue affecting both the environment and human societies worldwide. As a vital component of the hydrological cycle, groundwater serves as a critical source of water for agricultural, industrial, and residential purposes. However, the rapid increase in population intensified agricultural practices, industrial expansion, and climate change have significantly accelerated the rate of groundwater extraction, surpassing the natural replenishment rates. This unsustainable withdrawal groundwater not only threatens water security but also poses severe risks to ecosystems, agriculture, and the stability of human settlements. Understanding the causes, consequences, and mitigation strategies for groundwater depletion is imperative to ensuring the sustainable management of this invaluable resource and to maintain the balance of our environmental systems.

Extensive research has delved into the intricate problem of groundwater depletion, shedding light on its multifaceted nature and far-reaching impacts. The study by Wada et al. [19] emphasizes that agriculture is the primary driver of groundwater extraction, accounting for approximately 70% of global groundwater withdrawal. This heavy reliance on groundwater for irrigation is particularly evident in regions like northwest India, northeastern China, and the central United States, where intense agricultural activities lead to significant depletion rates . Similar findings are reported by Dalin et al. [5] who highlight the impact of international food trade on groundwater resources I exporting countries . Rodell et al. [15] also used satellite data to demonstrate the decline in groundwater levels due to decreased rainfall and increased evaporation rates, particularly in India. MacDonald et al. [11] describe how the growing demand for water in urban areas, coupled with industrial use, strains groundwater resources, leading to over-extraction and reduced availability for other uses. Famiglietti [6] and Perez et al. [14] emphasize that many regions are at risk of running out of accessible groundwater, which is crucial for drinking water supplies and sanitation. Groundwater depletion has severe environmental consequences. Excessive groundwater withdrawal can lead to decreased river flows, drying up of lakes and wetlands, and loss of biodiversity. Jasechko et al. [10] discuss how these environmental impacts further complicate the issue, as they affect ecosystems and the services they provide.

Fractional calculus, an extension of traditional calculus, deals with derivatives and integrals of non-integer orders. The application of fractional models across various disciplines demonstrates their versatility and effectiveness in addressing real-world problems (Boulaaras et.al. [3], Subramani et.al.[18], Meerschaert et.al.[12**])** By incorporating memory effects and long-range dependencies, fractional models provide a more accurate and comprehensive framework for understanding complex systems. Future research should focus on further refining these models and exploring new applications to enhance their utility in solving practical problems. Variable order fractional differential equation represents an advanced class of differential equations where the order of the derivative can change dynamically based on time, space, or other variables. This flexibility allows for more accurate modelling of complex systems exhibiting varying dynamical behaviour. These fractional variable-order operators have many applications in signal transmission, communicationtheory, hydrogeology, chemical kinetics, reaction theory, control systems, cryptography(Zhang & Chen [22], Wei, & Su [21], Atangana [1], Guo et.al.,[7], He & Yang [8]. Pandey et.al.,[13], Wang & Liu [20])

In view of the above, this study is driven by exploring how the variable-order fractional derivative is applied in contexts like Liouville-Caputo, Caputo-Fabrizio, and Atangana-Baleanu senses to analyse the behaviour of a model for groundwater depletion. The preliminary information for the fractional model is provided, offering a comprehensive explanation of the model in both its classical and fractional versions. The discussion includes the theoretical foundation and key differences between the classical and fractional approaches. A thorough analysis of the existence and uniqueness of fractional solutions is conducted, ensuring a solid mathematical basis for the model. Numerical results and simulations for the suggested model are presented. These results are obtained through detailed computational experiments, showcasing the model's accuracy and efficiency in various scenarios. Finally, all obtained results and findings are summarized and concluded in the final section.

II. PRELIMINARIES

This section provides some basic definitions of variable order fractional derivatives

Liouville–Caputo

The Liouville–Caputo (LC) fractional derivative with variable-order $\psi(\mathrm{t})$ is defined as

$${}^{LC}_{0}D_t^{\psi(\mathrm{t})}\, f(t) = \frac{1}{\Gamma 1-\psi(\mathrm{t})}\int_0^t (t-u)^{-\psi(\mathrm{t})} f(u)du\,,\ 0 < \psi(\mathrm{t}) \le 1$$

Caputo-Fabrizio

The Caputo–Fabrizio (CF) derivative with variable-order $\psi(\mathrm{t})$ in Liouville–Caputo sense is defined as follows

$${}^{CF}_{0}D_t^{\psi(\mathrm{t})} f(t) = \frac{(2-\psi(\mathrm{t}))M(\psi(\mathrm{t}))}{2(1-\psi(\mathrm{t}))}\int_0^t \exp[\frac{-\psi(\mathrm{t})}{(1-\psi(\mathrm{t}))}(t-u)]f'(u)du\ ,\ 0 < \psi(\mathrm{t}) < 1$$

where $M(\psi(\mathrm{t})) = \frac{2}{2-\psi(\mathrm{t})}$ is a normalization function.

Atangana-Baleanu

The Atangana–Baleanu (AB) fractional derivative with variable-order $\psi(\mathrm{t})$ in Liouville–Caputo sense is defined as follows

$${}^{AB}_{0}D_t^{\psi(\mathrm{t})} f(t) = \frac{B(\psi(\mathrm{t}))}{(1-\psi(\mathrm{t}))}\int_0^t E_{\psi(\mathrm{t})}[\frac{-\psi(\mathrm{t})}{(1-\psi(\mathrm{t}))}(t-u)^{\psi(\mathrm{t})}]f'(u)du\,,\ 0 < \psi(\mathrm{t}) \le 1$$

where $B(\psi(\mathrm{t})) = 1 - \psi(\mathrm{t}) + \frac{\psi(\mathrm{t})}{\Gamma\psi(\mathrm{t})}$ is a normalization function.

Remark: When $\psi(\mathrm{t})$ is a constant, then we retrieve the constant-order fractional derivative in Liouville-Caputo, Caputo-Fabrizio and Atangana-Baleanu sense

III. CLASSICAL MODEL OF GROUNDWATER LEVEL DECLINATION

A Mathematical model (M. A. Islam et al., [9]) is used to formulate the groundwater declination by the system of nonlinear equations. The three state variables considered by this model are as follows: A(t) signifies the atmospheric water level at time t, S(t) indicates the surface water level at time t, and G(t) represents the groundwater level at time t.

$$\frac{dA}{dt} = \lambda_1 S + \lambda_2 G - \alpha A - \gamma A$$

$$\frac{dS}{dt} = \alpha A - \beta GS - \lambda_1 S + \Phi GS + \omega G \qquad (1)$$
$$\frac{dG}{dt} = \beta GS - \lambda_2 G - \Phi GS - \omega G - \delta G$$

With initial conditions $A(0) = A_0$, $S(0) = S_0$, $G(0) = G_0$ and the total amount of water $N(t) = A(t) + S(t) + G(t)$. The parameter α represents the rate of precipitation from the atmosphere to surface water, while γ denotes the dissipation rate of atmospheric water. β indicates the infiltration rate from the surface to groundwater, and λ_1 and λ_2 refer to the rates of evaporation from surface and groundwater to atmospheric water, respectively. Surface water pollution rate is denoted by Φ. Moreover δ and ω signifies the rate of deforestation, and frequent pumping of water from ground level respectively.

IV. FRACTIONAL VERSION OF THE CLASSICAL MODEL

By substituting the classical derivative with the operator $\frac{d^{\psi(t)} f(t)}{dt}$, the fractional model of the system (1) is obtained.

$$\frac{d^{\psi(t)} A}{dt} = \lambda_1{}^{\psi(t)} S + \lambda_2{}^{\psi(t)} G - \alpha^{\psi(t)} A - \gamma^{\psi(t)} A$$
$$\frac{d^{\psi(t)} S}{dt} = \alpha^{\psi(t)} A - \beta^{\psi(t)} GS - \lambda_1{}^{\psi(t)} S + \Phi^{\psi(t)} GS + \omega^{\psi(t)} G \qquad (2)$$
$$\frac{d^{\psi(t)} G}{dt} = \beta^{\psi(t)} GS - \lambda_2{}^{\psi(t)} G - \Phi^{\psi(t)} GS - \omega^{\psi(t)} G - \delta^{\psi(t)} G$$

with initial conditions $A(0) = A_0, S(0) = S_0$, $G(0) = G_0$. The equilibria of the above fractional-order model can be obtained from

$$\frac{d^{\psi(t)} A}{dt} = 0 , \frac{d^{\psi(t)} S}{dt} = 0 \ \ and \ \ \frac{d^{\psi(t)} G}{dt} = 0$$

It was observed that the system (1) has two equilibria , one of them is pollution free and zero pumping ground water (i.e. $G = G_0$) equilibrium point $E_0 = (\bar{A}, \bar{S}, \bar{G})$ and the other one is general equilibrium point $E^* = (A^*, S^*, G^*)$
The Jacobian matrix of the system (2) is as follows

$$J = \begin{bmatrix} -\alpha^{\psi(t)} - \gamma^{\psi(t)} & \lambda_1{}^{\psi(t)} & \lambda_2{}^{\psi(t)} \\ \alpha^{\psi(t)} & -\beta^{\psi(t)} G - \lambda_1{}^{\psi(t)} + \Phi^{\psi(t)} G & -\beta^{\psi(t)} S + \Phi^{\psi(t)} S + \omega^{\psi(t)} \\ 0 & \beta^{\psi(t)} G - \Phi^{\psi(t)} G & \beta^{\psi(t)} S - \lambda_2{}^{\psi(t)} - \Phi^{\psi(t)} S - \omega^{\psi(t)} - \delta^{\psi(t)} \end{bmatrix}$$

The eigen values are the solutions of the characteristic equation $\det(A_i - \lambda I) = 0$.where the matrix A_i and the unit matrix I with the eigen values calculated at E_0 and E^*. For further details of the results can be found in (M.A. Islam et al. [9])

Since the parameters are dimensionless, the fractional models within LC, CF and AB sense will be the same and it will not be necessary to investigate again.

Existence and Uniqueness of Fractional solutions by the Liouville-Caputo model

Let us construct the system (2) as

$${}^{LC}_{0}D_t^{\psi(t)}[A(t)] = F_1(t, A) = \lambda_1{}^{\psi(t)} S + \lambda_2{}^{\psi(t)} G - \alpha^{\psi(t)} A - \gamma^{\psi(t)} A$$

$${}^{LC}_{0}D_t^{\psi(t)}[S(t)] = F_2(t, S) = \alpha^{\psi(t)} A - \beta^{\psi(t)} GS - \lambda_1{}^{\psi(t)} S + \Phi^{\psi(t)} GS + \omega^{\psi(t)} G \qquad (3)$$

$${}^{LC}_{0}D_t^{\psi(t)}[G(t)] = F_3(t, G) = \beta^{\psi(t)} GS - \lambda_2{}^{\psi(t)} G - \Phi^{\psi(t)} GS - \omega^{\psi(t)} G - \delta^{\psi(t)} G$$

By using Liouville-Caputo fractional integral operator to the above system, we get

$$A(t) - A(0) = \frac{1}{\Gamma\psi(t)} \int_0^t (t-k)^{\psi(t)-1} F_1(K, A(t))dk$$

$$S(t) - S(0) = \frac{1}{\Gamma\psi(t)} \int_0^t (t-k)^{\psi(t)-1} F_2(K, S(t))dk \qquad (4)$$

$$G(t) - G(0) = \frac{1}{\Gamma\psi(t)} \int_0^t (t-k)^{\psi(t)-1} F_3(K, G(t))dk$$

We will show that the kernel F_i for $i = 1,2,3$ follows the Lipschitz condition and contraction.

Theorem 1: The kernel F_i for $i = 1,2,3$ satisfies Lipschitz condition and contraction if the following inequality $0 \le r_i < 1$ holds.

Proof: Consider two functions $A \; and \; \bar{A}$

$$\|F_1(t, A) - F_1(t, \bar{A})\|$$

$$= \left\| {\lambda_1}^{\psi(t)} S + {\lambda_2}^{\psi(t)} G - \alpha^{\psi(t)} A - \gamma^{\psi(t)} A - ({\lambda_1}^{\psi(t)} S + {\lambda_2}^{\psi(t)} G - \alpha^{\psi(t)} \bar{A} - \gamma^{\psi(t)} \bar{A}) \right\|$$

$$= \left\| -(\alpha^{\psi(t)} + \gamma^{\psi(t)})(A - \bar{A}) \right\|$$

$$\le \left\| \alpha^{\psi(t)} + \gamma^{\psi(t)} \right\| \|(A - \bar{A})\|$$

$$\le r_1 \|A - \bar{A}\| \qquad (5)$$

where $r_1 = \left[\alpha^{\psi(t)} + \gamma^{\psi(t)}\right]$ is a positive constant. As a result, the Lipschitz condition is met for $r_1$and if $0 \le r_1 < 1$, then $r_1$follows contraction. Similarly, it can be exihibited and demonstrated in the other equations as follows

$$\|F_2(t, S) - F_2(t, \bar{S})\| \le r_2 \|S - \bar{S}\|$$

$$\|F_3(t, G) - F_3(t, \bar{G})\| \le r_3 \|G - \bar{G}\|$$

Therefore F_i satisfies Lipschitz condition.Also, if $0 \le r_i < 1$, then the kernels follows contractions.

From system (3), the recurrent form can be written as follows

$$\Phi_{1n} = A_n(t) - A_{n-1}(t) = \frac{1}{\Gamma\psi(t)} \int_0^t (t-k)^{\psi(t)-1} [F_1(K, A_{n-1}) - F_1(K, A_{n-2})]dk$$

$$\Phi_{2n} = S_n(t) - S_{n-1}(t) = \frac{1}{\Gamma\psi(t)} \int_0^t (t-k)^{\psi(t)-1} [F_2(K, S_{n-1}) - F_2(K, S_{n-2})]dk$$

$$\Phi_{3n} = G_n(t) - G_{n-1}(t) = \frac{1}{\Gamma\psi(t)} \int_0^t (t-k)^{\psi(t)-1} [F_3(K, G_{n-1}) - F_3(K, G_{n-2})]dk$$

Now taking norm for $\|\Phi_{1n}(t)\|$, we get

$$\|\Phi_{1n}(t)\| = \|A_n(t) - A_{n-1}(t)\| = \left\| \frac{1}{\Gamma\psi(t)} \int_0^t (t-k)^{\psi(t)-1} [F_1(K, A_{n-1}) - F_1(K, A_{n-2})]dk \right\|$$

$$\leq \frac{1}{\Gamma\psi(t)}\int_0^t \left\|(t-k)^{\psi(t)-1}[F_1(K,A_{n-1})-F_1(K,A_{n-2})]\right\| dk$$

Now using Lipschitz condition in the above equation, we obtain

$$\|\Phi_{1n}(t)\| \leq \frac{r_1}{\Gamma\psi(t)}\int_0^t \|\Phi_{1(n-1)}(k)\| dk$$

Similarly

$$\|\Phi_{2n}(t)\| \leq \frac{r_2}{\Gamma\psi(t)}\int_0^t \|\Phi_{2(n-1)}(k)\| dk$$

$$\|\Phi_{3n}(t)\| \leq \frac{r_3}{\Gamma\psi(t)}\int_0^t \|\Phi_{3(n-1)}(k)\| dk \qquad (6)$$

which implies that it can be written as

$$A_n(t) = \sum_{i=1}^n \Phi_{1i}(t)\,,\, S_n(t) = \sum_{i=1}^n \Phi_{2i}(t),\, G_n(t) = \sum_{i=1}^n \Phi_{3i}(t)$$

Theorem 2:[16] The Liouville -Caputo model (3) has system of solutions if there exists t >1 such that $\frac{r_i t}{\Gamma\psi(t)} \leq 1$ for i=1,2,3

Theorem 3:[16] If the condition $\left[1-\frac{r_i t}{\Gamma\psi(t)}\right] \geq 0$, for $i = 1,2,3$ holds then Liouville-Caputo model have unique solution.

Similarly we establish existence and uniqueness of fractional solutions by Caputo-Fabrizio and Atangana-Baleanu [16].

V. NUMERICAL SCHEME

In this section, the Numerical scheme (Solís-Pérez et al.[17])is considered in the sense of Liouville-Caputo, Caputo-Fabrizio and Atangana –Baleanu fractional derivatives.
Let us consider our fractional model as

$${}_0^*D_t^\alpha u(t) = f(t,u(t))$$

Where * denotes LC, CF and AB terms and $u(t) = (A(t), S(t), G(t))$.
Now we use the numerical scheme represented for Liouville-Caputo (7), Caputo-Fabrizio(8) and Atangana-Baleanu (9) fractional derivatives in (2)

$$u_{n+1}(t) = u(0) + \frac{1}{\Gamma\psi(t)}\sum_{m=0}^n \left(\begin{array}{c} \frac{h^{\psi(t)} f(t_m,u_m)}{\psi(t)(\psi(t)+1)} \\ ((n-m+2+2\alpha) - \frac{h^{\psi(t)} f(t_{m-1},u_{m-1})}{\psi(t)(\psi(t)+1)} \\ \left(\begin{array}{c}(n+1-m)^{\psi(t)+1} - \\ (n-m)^{\psi(t))}(n-m+1+\psi(t)\end{array}\right) \end{array}\right) \qquad (7)$$

$$(u_{n+1}) = (u_n) + \left[\begin{array}{c}\frac{(2-\psi(t))(1-\psi(t))}{2} \\ +\frac{3h}{4}\psi(t)(2-\psi(t))\end{array}\right] f(t_n,u_n) + \left[\begin{array}{c}\frac{(2-\psi(t))(1-\psi(t))}{2} + \\ \frac{h}{4}\psi(t)\,(2-\psi(t))\end{array}\right] f(t_{n-1},u_{n-1}) \quad (8)$$

$$u_{n+1}(t) = u(0) + \frac{\Gamma\psi(t)(1-\psi(t))}{\Gamma\psi(t)(1-\psi(t))+\psi(t)} f(t_n,u_n) +$$

$$\frac{1}{(\psi(t)+1)\big((1-\psi(t))\,\Gamma\psi(t)\big)+\psi(t)}\sum_{m=0}^{n}\begin{pmatrix} h^{\psi(t)}f(t_m\,,u_m) \\ \begin{pmatrix}(n+1-m)^{\psi(t)}\,(n-m+2+\psi(t)) \\ -\,(n-m)^{\psi(t)}(n-m+2+2\alpha(t)\end{pmatrix} \\ -h^{\psi(t)}f(t_{m-1}\,,u_{m-1}) \\ \begin{pmatrix}(n+1-\ m)^{\psi(t)+1} \\ -\,(n-m)^{\psi(t)}\ \ (n-m+1+\psi(t))\end{pmatrix}\end{pmatrix} \tag{9}$$

VI. RESULTS AND DISCUSSION

The primary goal of our proposed fractional model is to investigate the impact of deforestation, pollution, evaporation, and frequent pumping on the decline in groundwater levels, taking into account various variables and fractional orders. This model aims to provide a more nuanced understanding of these factors by incorporating fractional calculus, which allows for the modeling of memory and hereditary properties of the processes involved.

According to the hydrological cycle, water evaporates from oceans and land surfaces, entering the atmosphere as water vapour. This vapour then travels through the atmosphere, where it eventually condenses and precipitates back onto the surface or into the oceans. In areas with vegetation, precipitation can be intercepted by plant leaves, contributing to surface runoff. This runoff seeps into the ground, replenishing underground water reserves, and eventually reaches streams and rivers as surface runoff. The intercepted water and surface runoff re-enter the atmosphere through direct evaporation from the soil and vegetation or through transpiration from plant leaves, maintaining the continuous cycle of the water system. Our model examines how disruptions in this cycle, caused by human activities such as deforestation and pollution, or natural processes like evaporation and pumping, lead to changes in groundwater levels. By considering fractional orders, the model captures the complexity and interconnectedness of these processes over time, providing a deeper insight into groundwater dynamics and offering potential strategies for sustainable water resource management.

The decline of atmospheric, surface, and groundwater resources is driven by various interconnected factors. Climate change is the primary driver behind the decrease in atmospheric water. This phenomenon leads to shifts in rainfall patterns and elevated temperatures. Deforestation also plays a significant role by diminishing transpiration, resulting in a reduction of water vapor. The impact of air pollution further exacerbates this issue by interfering with cloud formation, resulting in a notable depletion of water in the atmosphere. Surface water depletion is also a result of climate change, which changes patterns of rainfall and increases evaporation rates. Additionally, excessive usage for agricultural, industrial, and residential purposes contributes to the decline. Pollution impairs water quality, while the expansion of urban areas and agricultural practices disrupt the natural flow of water and diminish its replenishment. Groundwater decline is driven by over-extraction for irrigation, industry, and drinking water. Climate change reduces precipitation and increases evaporation which, further decreasing recharge. Urbanization and deforestation reduce infiltration areas, while pollution from agricultural chemicals, industrial waste, and septic leaks contaminate groundwater.

Addressing groundwater decline involves integrated water management, sustainable resource use, pollution control, and climate change adaptation. This includes efficient allocation, water-saving technologies, runoff regulation, resilient infrastructure, and diversifying water sources to ensure sustainability and protection of groundwater. Groundwater systems possess considerable memory effects because they rely on historical inputs and past conditions. This indicates that the current groundwater levels are not only impacted by present circumstances but also by previous events and interactions. Conventional integer-order models often struggle to accurately depict these relationships, while fractional order models excel at capturing this aspect.

Case 1(Variable-order case): The level of Atmospheric water changes over time takes the variable order as $\psi(\mathrm{t})$ =P.exp(−k.t),where P indicates the atmospheric water content, it depends on temperature variations and humidity levels and k represents the declination of the atmospheric water content over time t. S(t) takes the variable order as $\psi(\mathrm{t})$=1-exp(-r.t),where 1 represents the function will eventually capture the entire response(i.e. total runoff, complete infiltration, or maximum evaporation rate) and R indicates the speed of the response. The variable order of G(t) can be represented by the function $\psi(\mathrm{t}) = 1/(1+\exp(\lambda(\mathrm{t}-\nu))$,here λ represents the growth rate of groundwater level and ν indicates the midpoint or Inflection Point ,that is ,the point where the function is increasing most rapidly and is halfway between its initial and final values.

Figures 1, 2, 3 represents the above discussed variable-order Fractional forms of A(t),S(t) and G(t) in LC,CF and AB senses by taking possible parameter values from the literature. We utilized the MATLAB R2023a programming language to perform numerical simulations of our fractional model.

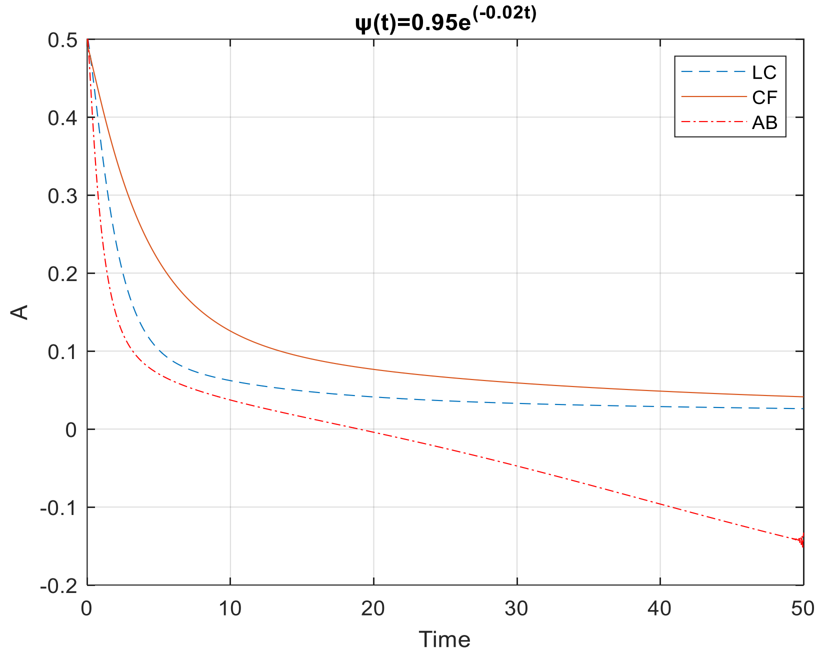

Fig.1 Comparison graph of Atmospheric water level via LC, CF and AB

Figure 1 illustrates the level of atmospheric water with a variable order represented by ψ(t)=0.95exp(-0.02t). Here, 0.95 denotes the atmospheric water content and 0.02 represents their declination rate. It is noted that the level of atmospheric water decreases eventually and stable in our considered time as in case of LC and CF, whereas AB predicts the fastest depletion and crossing below zero, it is quite unusual for natural occurrences.

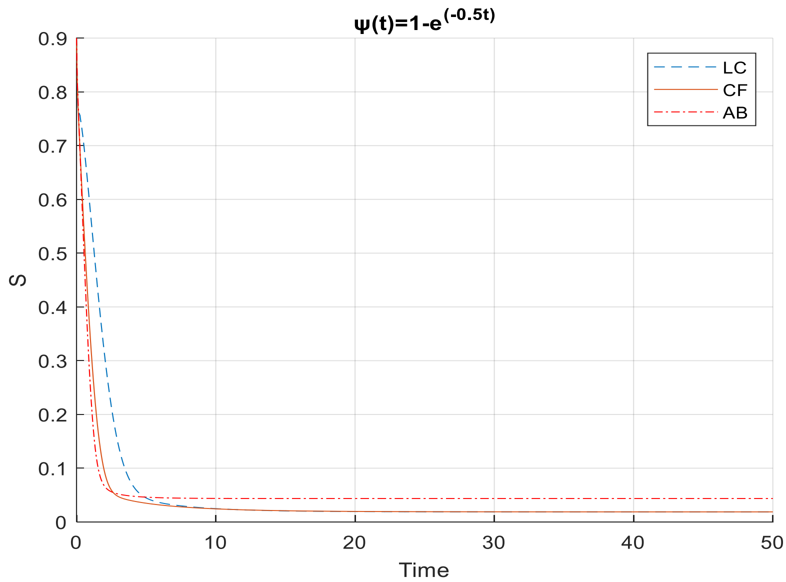

Fig. 2 Comparison graph of Surface water level via LC, CF and AB

Figure 2 depicts the surface water level by the variable order as $\psi(t)$=1-exp(-0.5t), here 1 indicates the realization of entire potential effect and 0.5 represents the rate of the response. It is observed that, the level of surface water decreases rapidly and stabilizes more closely in case of LC and CF than AB.

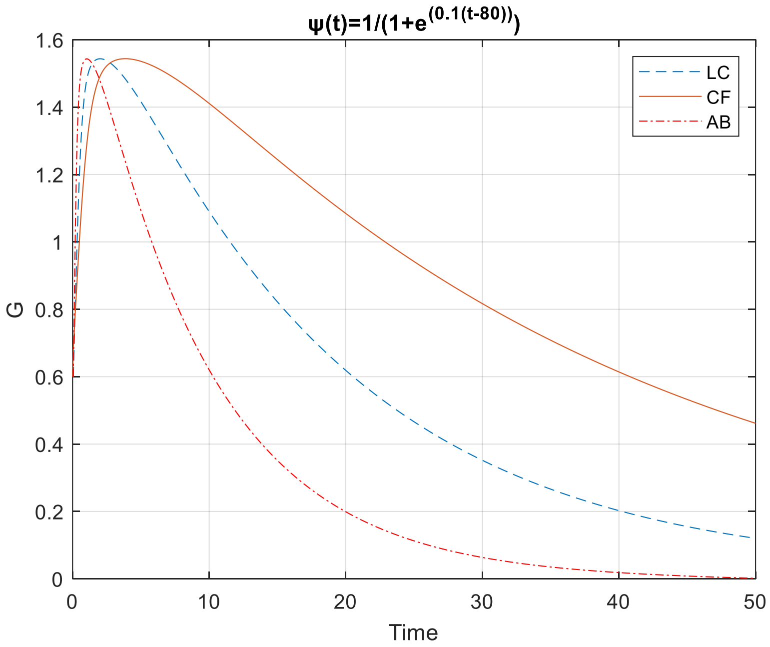

Fig. 3 Comparison graph of Groundwater level via LC, CF and AB

Figure 3 provides a graph of the variable order function $\psi(t) = 1/(1 + \exp(0.1(t - 80))$, where 0.1 represents the increasing rate of groundwater level and 80 indicates the midpoint or inflection point. Using LC, CF and AB for observing the considered function, the level of groundwater decreases and comes to saturation level more quickly in AB than in LC and CF.

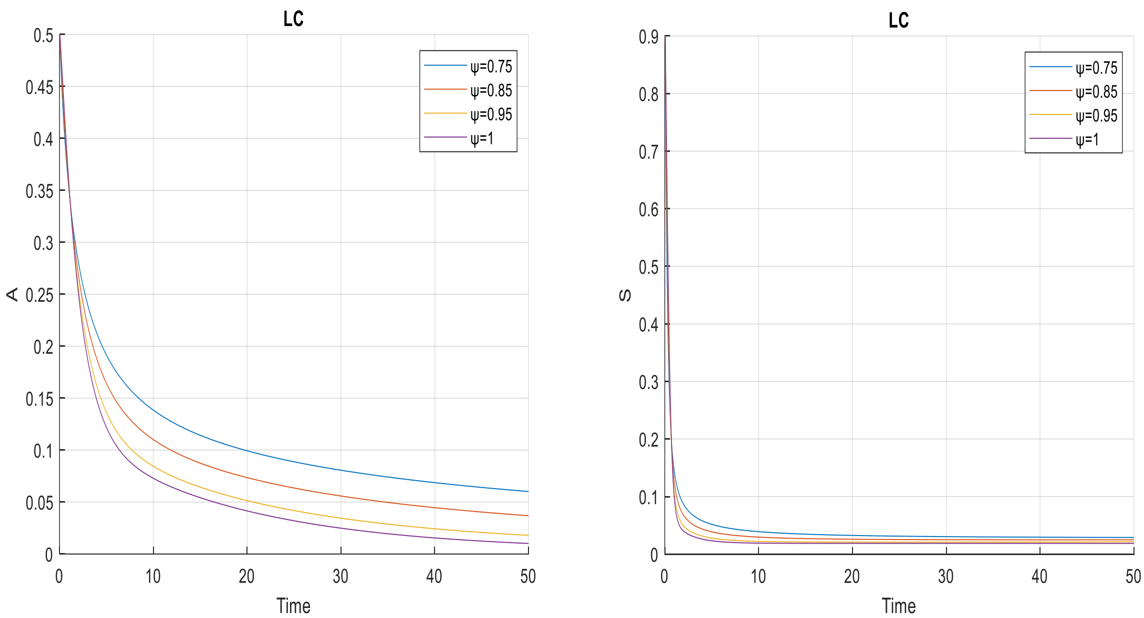

(a) (b)

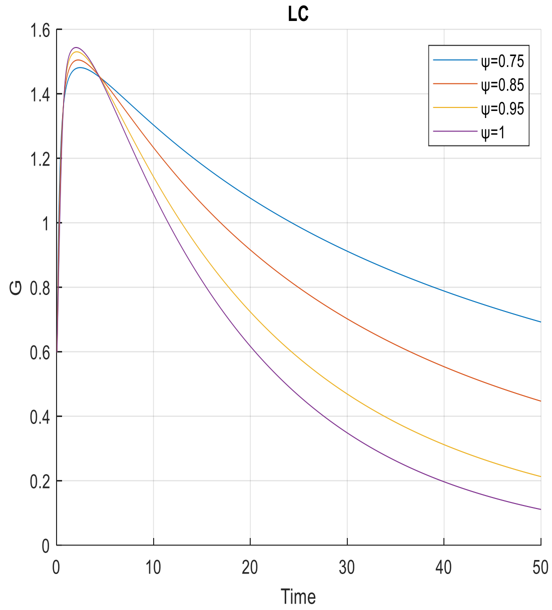

(c)

Fig.4 Numerical Simulations for various order of ψ at 0.75,0.85,0.95 and 1 in Liouville-Caputo sense

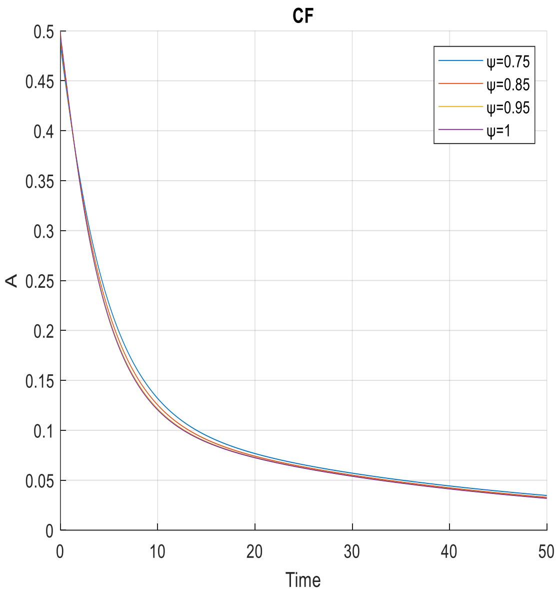

(a)

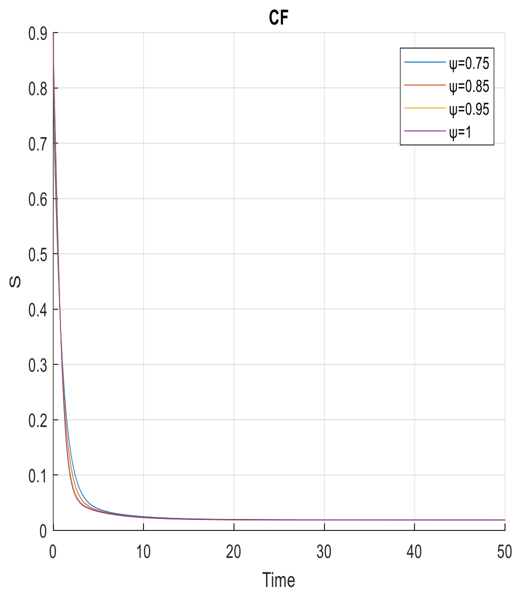

(b)

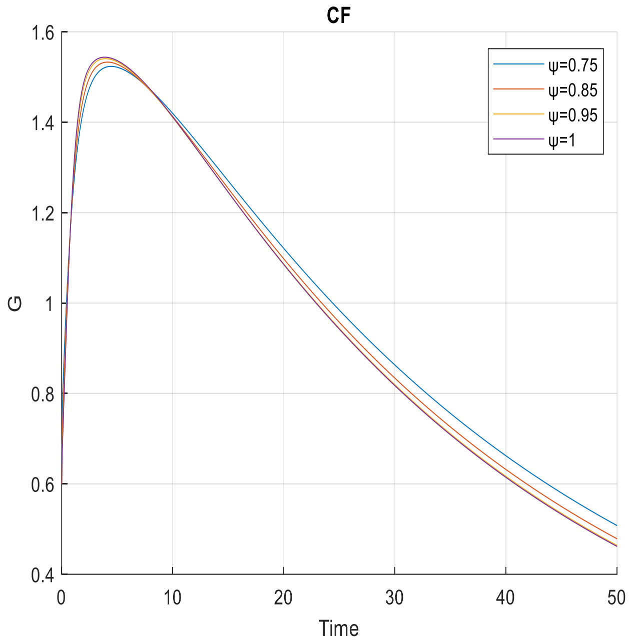

(c)

Fig.5 Numerical Simulations for various order of ψ at 0.75, 0.85,0.95 and 1 in Caputo-Fabrizio sense

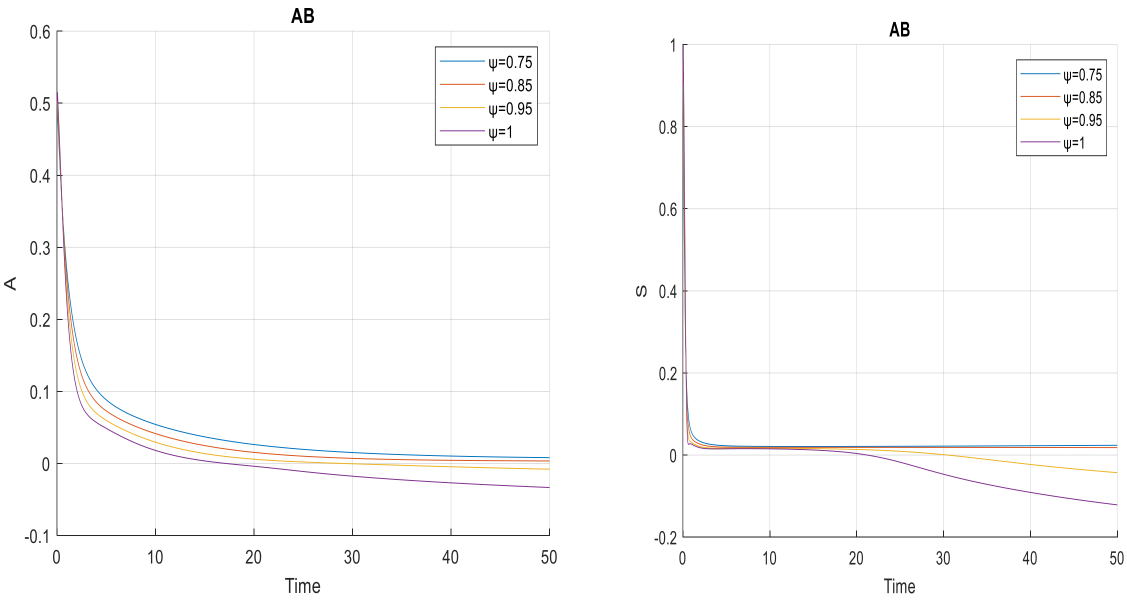

(a) (b)

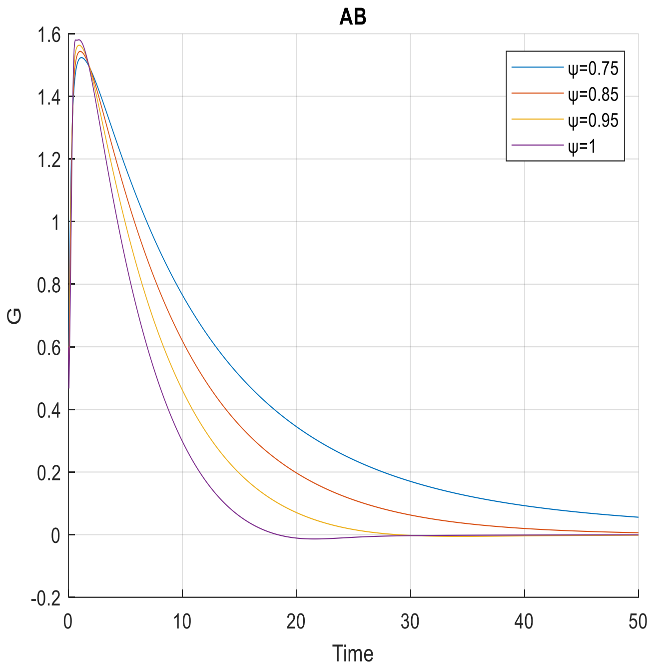

(c)

Fig.6 Numerical Simulations for various order of ψ at 0.75,0.85,0.95 and 1 in Atangana-Baleanu sense.

Case 2 (Fractional-order case): Figures 4, 5, 6 depicts the numerical simulation of $A(t)$, $S(t)$ and $G(t)$ for various fractional values 0.75,0.85,0.95 and 1 of Liouville-Caputo, Caputo-Fabrizio and Atangana-Baleanu models respectively.

Figures 4 and 6 shows that the declination of atmospheric water level increases gradually as ψ approaches 1 as in case of LC and AB but in CF (Figure 5) ,the increasing value of ψ, not impact much in the declination level of atmospheric water. Figures 4 and 5, demonstrates that the surface water level decreases rapidly and stable for increasing value of ψ whereas Figure 6 shows a deviation in the stabilization as ψ value of AB increases. Figure 4 illustrates a gradual decline in groundwater level for increasing ψ values. The rise in value ψ results in a gradual decline in the groundwater level for LC (Figure 4), a closer decline for CF(Figure 5), and an equilibrium state for AB(Figure 6).

As from the literature [5,6,10,11,14,15,19] it seems that for variable order case the results of LC and CF are more reliable when compared to AB. For fractional–order case, it is observed that LC has better memory effect than CF and AB. Since CF have minimum variations for increasing value of ψ and AB deviates from the saturation level when ψ approaches to 1.

VI. CONCLUSION

In this research, a non-linear fractional variable-order model is introduced for the decline of groundwater levels, incorporating Liouville-Caputo, Caputo-Fabrizio, and Atangana-Baleanu fractional derivatives. Through numerical simulations, the model illustrates the significant influence of deforestation, pollution, evaporation, and excessive water extraction on groundwater reserves. These insights emphasize the necessity for integrated water management strategies, sustainable resource use, and pollution control to address groundwater decline effectively. Our findings underscore the importance of selecting appropriate fractional models to capture the complex dynamics of groundwater systems, ensuring more accurate predictions and better-informed decision-making for water resource management.

REFERENCES

[1] Atangana, On the stability and convergence of the time-fractional variable order telegraph equation. *J. Comput. Phys.*, ***293*** (2015) 104–114.

[2] M.H.A. Biswas, T. Rahman, & N. Haque, Modeling the potential impacts of global climate change in Bangladesh: An optimal control approach. *J. Fundam. Appl. Sci.*, ***8*****(1)** (2016)1-19.

[3] S. Boulaaras, F. Alharbi, T. Kone, & A.M. Wazwaz, SEIR model for COVID-19: Stability of the standard coronavirus factor and control mechanism. *Mathematics*, ***11*****(1)** (2023) 21.

[4] H. Brammer & P. Ravenscroft Arsenic in groundwater: A threat to sustainable agriculture in South and South-East Asia. *Environment International*, ***35*****(3)** (2009) 647-654.

[5] C. Dalin, Y. Wada, T. Kastner, & M.J. Puma, Groundwater depletion embedded in international food trade, *Nature, **543***(**7647**) (2017) 700-704.
[6] J.S. Famiglietti , The global groundwater crisis. *Nature Climate Change, **4***(**11**) (2014) 945-948.
[7] Y.M. Guo, Y. Zhao, Y.M. Zhou, Z.B. Xiao, & X.J. Yang, On the local fractional LWR model in fractal traffic flows in the entropy condition. *Math. Methods Appl. Sci., **40***(**17**) (2017) 6127–6132.
[8] J. He & X. Yang, Variable-order fractional calculus in modeling complex chemical reactions. *Chemical Engineering Science, **249*** (2024)117413.
[9] Md. A. Islam & Md. H.A. Biswas, Potential impact of climate change on groundwater level declination in Bangladesh: A mathematical modelling computation. *Informatica, **47*** (2023) 261-274.
[10] S. Jasechko, H. Seybold, D. Perrone, Y. Fan, M. Shamsudduha, R.G. Taylor, O. Fallatah, and J.W. Kirchner, Rapid groundwater decline and some cases of recovery in aquifers globally, *Nature, **625***(**7996**) (2024) 715-721.
[11] A.M. MacDonald, H.C. Bonsor, B.É. Ó Dochartaigh, & R.G. Taylor, Quantitative maps of groundwater resources in Africa. *Environmental Research Letters, **7***(**2**) (2016) 024009.
[12] M.M. Meerschaert & H.P. Scheffler Limit theorems and stable processes for truncated Lévy flights. *Journal of Applied Probability, **38***(**2**) (2001) 213-228.
[13] S. Pandey, N.K. Soni, & R.K. Pandey. A study on variable-order fractional PID controllers for robust control systems. *Journal of Vibration and Control, **30***(**2**) (2024) 143-159.
[14] N. Perez, V. Singh, C. Ringler, H. Xie, T. Zhu, E.H. Sutanudjaja, & K.G. Villholth Ending groundwater overdraft without affecting food security. *Nature Sustainability, **7***(**8**)(2024)1007-1017.
[15] M. Rodell, I. Velicogna, & J.S. Famiglietti Satellite-based estimates of groundwater depletion in India. *Nature, **460***(**7258**) (2009) 999-1002.
[16] T. Saradhadevi, A. Kalavathi, N. Punitha, & A. Saranya, A novel mathematical investigation of synthetic precipitation employing diverse variable-order nonlinear fractional derivatives. *Advances in Nonlinear Variational Inequalities, **27***(**2**) (2024)78-101.
[17] J.E. Solís-Pérez, J.F. Gómez-Aguilar, & A. Atangana , Novel numerical method for solving variable-order fractional differential equations with power, exponential and Mittag-Leffler laws. *Chaos, Solitons and Fractals, **114*** (2018)175-185.
[18] R. Subramani, B. Balachandran, & R. Raja, The dynamic analysis of discrete fractional-order two-gene map. *Mathematics, **11***(**2**) (2023)156.
[19] Y. Wada, L.P.H. van Beek, C.M. van Kempen, J.W.T.M. Reckman, S. Vasak, & M.F.P. Bierkens, Global depletion of groundwater resources. *Geophysical Research Letters, **37***(**20**) (2010).
[20] L. Wang & H. Liu, Enhancing cryptographic algorithms using variable-order fractional operators. *Entropy, **26***(**1**) (2024)110.
[21] Y. Wei & D. Su, Modeling groundwater contaminant transport using variable-order fractional operators. *Journal of Hydrology, **613*** (2024) 128047.
[22] Y. Zhang & Y. Chen, Applications of variable-order fractional differential equations in signal processing and communication systems. *IEEE Transactions on Signal Processing, **72***(**5**) (2024) 1245-1260.